Tutrace: Editable Animated Vector Shape from Video

Loïc Vital[a]
Technicolor Group, France

Keywords: Video, Vectorization, Rotoscopy, Animation, Vector Graphics.

Abstract: We present a new video vectorization technique for converting a sequence of binary images into an animated vector shape. Our approach offers the benefit of producing an output that can be directly used in a compositing software to apply manual edits and corrections, which is often a mandatory constraint for rotoscoping artists in the VFX industry. Our process initially builds a frame-by-frame vectorization of the input, finds correspondences between vertices at different frames, and extracts an animated vector shape from the induced graph structure. Although the presented method is completely automatic, the general approach is flexible and offers several controls to adjust the fidelity vs. simplicity trade-off in the generated output.

1 INTRODUCTION

In the visual effects (VFX) industry, rotoscoping artists work primarily with animated shapes (closed or open 2D curves) as these vector graphics primitives provide fine control over the final result and allow re-editing in case of feedback from clients, supervisors or downstream departments. However, using these animated shapes comes at a cost, as they require several hours of careful manual work from trained artists to be initially created.

On the other hand, image segmentation methods have matured in the recent years, and it is now possible to automatically extract a desired object from a video with great precision in a number of scenarios. However the lack of control and ability to edit the results is currently making it difficult for VFX studios to integrate these methods in their standard workflow.

In this work, we propose a method to bridge this gap, i.e. turn a segmented video (made out of binary images) into an animated vector shape, which can be imported in a compositing DCC[1] such as Nuke or Silhouette for re-editing. We call this method *Tutrace*. This name originated as a blend between the initial inspiration for the algorithm, *Potrace*, and the topology of the output, which resembles a *tube* or *tunnel*.

The fact that we are targeting DCC-compatible animated vector shapes imposes some specific constraints on the structure of the output. More precisely, this means we must produce closed curves whose geometry is specified by a set of keyframes, i.e. frame values along the timeline where the positions of all control points are prescribed. Using this representation, the curve geometry in-between two keyframes is determined by interpolating the control points positions.

The main challenge imposed by this structure is that the number of vertices is fixed for the entire frame range. By contrast, applying a single-image vectorization algorithm to each frame independently would create vector shapes with a varying number of vertices, adapted to the input geometry. This is particularly visible in areas where details appear or disappear over the animation: a flat area needs only two vertices to be represented, but if this area breaks into several parts then more vertices are needed.

Our algorithm works by first vectorizing each video frame independently, then finding correspondences between these initial static vector shapes to extract an animated vector shape, and finally simplifying it. Our main contribution lies in the central part of this algorithm, which is the process of going from a sequence of static vector shapes to an animated vector shape, thus solving the problem stated above using an *ad-hoc* method. The simplifications performed afterwards on the animated shape aim at reducing its complexity, i.e. the number of animated vertices and keyframes, thus making the output better suited for manual editing.

[a] https://orcid.org/0009-0002-7972-9242

[1] Digital Content Creator, i.e. software dedicated to creating and editing digital content such as 2D/3D geometry, images, etc.

Vital, L.
Tutrace: Editable Animated Vector Shape from Video.
DOI: 10.5220/0013097900003912
Paper published under CC license (CC BY-NC-ND 4.0)
In *Proceedings of the 20th International Joint Conference on Computer Vision, Imaging and Computer Graphics Theory and Applications (VISIGRAPP 2025) - Volume 1: GRAPP, HUCAPP and IVAPP*, pages 19-28
ISBN: 978-989-758-728-3; ISSN: 2184-4321
Proceedings Copyright © 2025 by SCITEPRESS – Science and Technology Publications, Lda.

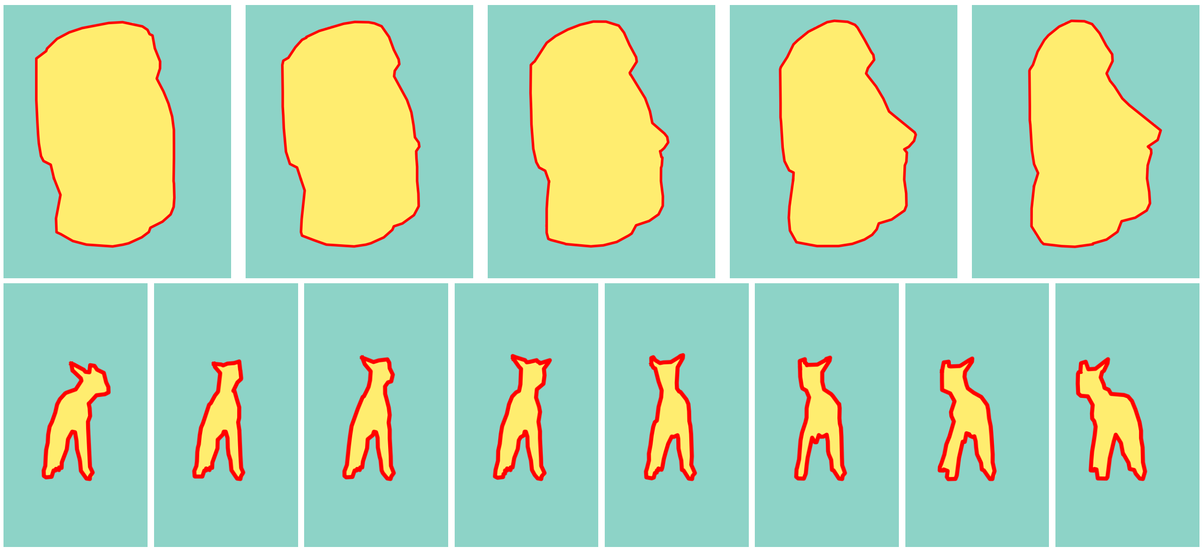
Figure 1: Animated vector shapes generated by Tutrace on the “statue” (first row) and “sheep” (second row) sequences, shown in red and overlaid on the images.

2 RELATED WORK

2.1 Video Object Segmentation

Image segmentation and object segmentation in video are fundamental problems in computer vision, and there is now extensive literature on that topic (Yu et al., 2023) (Yao et al., 2020). Going from object segmentation in a single image to a sequence of images is not a trivial task, as temporal coherence has to be taken into account, and many artifacts can arise.

In this article, we do **not** present any new segmentation method: this work is *complementary* to segmentation, as it takes a binary image sequence as input and produces an animated vector shape. The motivation behind this is to provide users with direct control over the results of an automatic segmentation process, rather than relying on implicit controls.

2.2 Image Vectorization

There has been much work on single-image vectorization, with various algorithms and representations proposed to cover a wide range of inputs: natural images, cartoon, manga, line drawings (Favreau et al., 2016), and even pixel art (Kopf and Lischinski, 2011).

These methods can be classified into two main categories depending on the representation they work with, namely meshes or curves. Mesh-based methods span a wide range of primitives, including Ferguson patches (Sun et al., 2007) and triangular Bézier patches (Xia et al., 2009). The curve-based methods also include various primitives, for instance closed polygons and Bézier curves (Selinger, 2003) as well as diffusion curves (Orzan et al., 2008).

In this work, we focus particularly on the context of rotoscopy, thus adding the constraint that we must be able to import and edit the vectorization result in a compositing DCC. Therefore the set of possible primitives we can use is reduced to closed curves, thus making Potrace (Selinger, 2003) an adequate choice to base our work on.

2.3 Video Vectorization

Several methods have already been proposed for video vectorization, however they do not focus on the same objectives as we do.

(Zhang et al., 2009) proposes a method specifically tailored for cartoon animation, and focuses on decomposing the input images into spatially and temporally coherent regions. However the final output it generates is a frame-by-frame vectorization, not an animated shape.

(Wang et al., 2017) takes a quite different approach: it considers the input video as a volume with color information, and the vectorization as a tetrahedral meshing problem. This approach greatly simplifies the spatial-temporal duality and offers a link between vectorization and the wide literature on mesh processing, however the output it generates is a tetrahedral mesh, which is not usable in any compositing DCC and not easily convertible into an animated shape.

(Li et al., 2021) proposes a method based on diffusion curves, producing results of great visual quality, using a combination of optical flow and shape matching techniques for temporal coherence. However once again the output is not an animated shape, but a frame-by-frame vectorization. In addition, the output is made out of diffusion curves, which do not have any topology constraint, and therefore generally do not form a closed curve, therefore making the output of this algorithm unfit to be used in ours.

(Zhang et al., 2023) focuses on *motion graphics video*, i.e. animated graphic designs. They address the problem of motion tracking and layered decomposition, which is of critical importance whenever multiple objects are in the scene. The output they produce, however, is not a vector shape: each tracked object is associated with an image inferred from the video input, called its *canonical image*, a sequence of per-frame affine transforms and a sequence of per-frame z-index depth. In particular, this representation implies that their approach does not handle *change* in the objects themselves, such as details appearing and disappearing throughout the animation, which occurs quite frequently in the context of rotoscopy and must not be put aside.

3 MOTIVATION AND OVERVIEW

3.1 Problem Statement

The input data we consider in this work is a finite sequence of images $(I_f)_{0 \leq f < F}$ where F is the number of frames. All these images share the same dimensions (w,h). In this article we do not take color into account, we only treat *binary* images, i.e. images with pixel values in the set $\{0,1\}$.

We also make another strong assumption on these images: we assume that in each image, the pixels with value 1 form a connected component without hole. We call this component the *content* of the image. This assumption greatly simplifies the topology of the animated content.

The output we want to produce is an animated shape, i.e. a closed curve defined by a sequence of N vertices animated over K keyframes. Each keyframe defines a fixed 2D position for the vertices, and for a given frame in-between two keyframes the vertices positions are linearly interpolated to determine the shape geometry on that frame. Note that such an animated shape is not necessarily a polygon: the vertices could also be interpreted as control points for a smooth curve. However, in the work that follows, we will focus on generating an animated polygon.

3.2 Algorithm Breakdown

The overall workflow of the algorithm is quite intuitive: we start by vectorizing each image independently, then we match the vertices between consecutive frames to create animated vertices, thus forming an animated shape.

However most single-image vectorization algorithms will try to simplify the shape geometry by removing vertices in “flat” areas, which is problematic for the matching phase. Indeed, if a portion of the shape is flat at a given frame but “breaks into two parts” at the following frame, hence creating a new vertex at the breaking point, we won’t be able to match this new vertex against the shape at the first frame (see Figure 3a). To overcome this issue, we make sure that the first vectorization step produces a sequence of densely sampled shapes (see Figure 3b) and we delay the simplification step until the end of the algorithm, when we have a fully animated shape. We refer to this final simplification step as *pruning*.

In addition, it is quite likely that the matching phase does not produce 1-to-1 vertex matches between consecutive frames, which makes the process of creating animated vertices and joining them into an animated shape more complex than simply chaining the matches. We call this process *untangling*.

In summary, our algorithm follows these four steps, depicted in Figure 2: extract a *dense contour* from each image, match the vertices of these contours between consecutive frames, untangle these matches to produce an animated shape, and prune the animated vertices and keyframes on this animated shape.

3.3 Data Structure

The data structure we use in our method is a simplified version of the work presented in (Dalstein et al., 2015), which we will call a *Tutrace complex*.

At the most abstract level, a Tutrace complex is just a directed graph. A node in this graph is called a *key vertex*, and it encodes both a 2D position and a frame number. As for the edges in this graph, they are split into two categories: the *key edges* and the *temporal edges*. A key edge always links two key vertices which have the same frame number, whereas a temporal edge always links two key vertices with different frame numbers, and is directed from lower to higher frame number.

This graph structure is enriched with additional entities which provide higher-level structures and semantic for working with a Tutrace complex. A *key cycle* is a looping path of key edges, and can be seen as a static vector shape (made out of a single closed

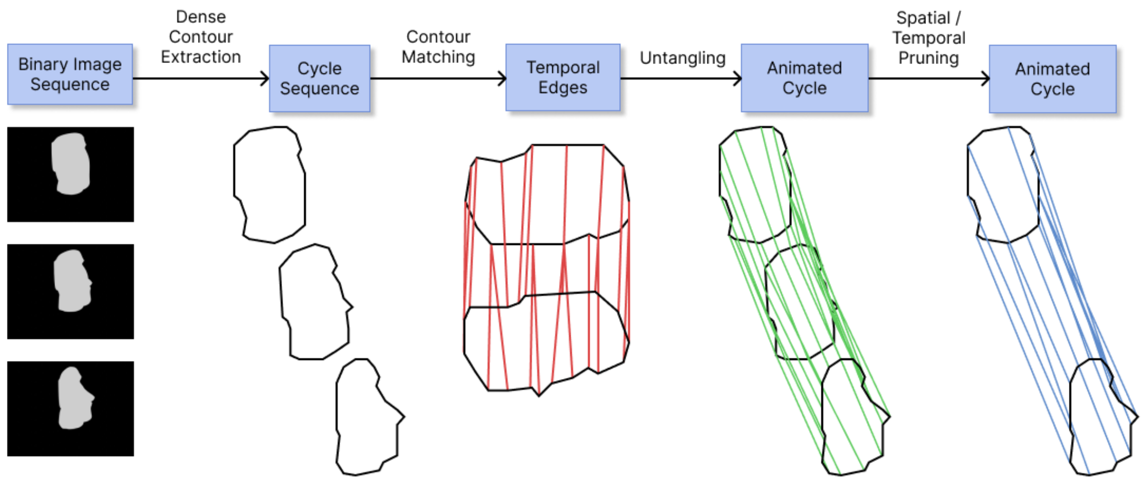

Figure 2: Overview of the Tutrace algorithm.

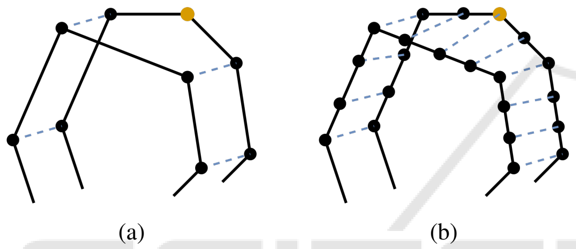

Figure 3: Contour matching. Solid lines represent contours and dashed lines represent matches. (a) Sparse contour. In this case, there is no good candidate vertex to match the highlighted vertex. (b) Dense contour. Here, finding a good match for the each vertex becomes possible.

curve). A key cycle naturally inherits the frame number of its key edges. A sequence of key cycles with increasing frame numbers is called a *cycle sequence*. An *animated vertex* is a path of temporal edges. A circular sequence of animated vertices is called an *animated cycle*, and can be seen as an animated vector shape.

4 DENSE CONTOUR

The first step of our algorithm is the extraction of dense contours. This routine will run on each image separately, and is very similar to a single-image vectorization algorithm, the main difference being that we wish to keep a dense and regular sampling of points along the resulting shape.

4.1 Contour Extraction

For a given image, this phase begins by tracing the image's *content*, i.e. it generates a closed polygon curve that follows the boundary of the content's pixels (see Figure 4a).

This polygon is the most densely sampled shape we can get, however since it follows the exact border of the pixels it also contains some high-frequency details that we would like to get rid of (staircase effect) as they do not play a part in the actual shape we perceive.

4.2 Contour Simplification

We add to this first tracing step a *constrained simplification* step, i.e. a simplification step that obeys the following constraints: for any two consecutive points p,q on the output polygon, $||p-q||_2 < d_{max}$, with d_{max} a parameter of the algorithm (see Figure 4b).

To perform this constrained simplification we decided to use an iterative algorithm that progressively decimates edges on the polygon while always respecting the constraint. The decimation is done by using a 2D adaptation of the edge-contraction technique based on quadric error metric, introduced in (Garland and Heckbert, 1997). However, we add an eligibility condition on edges: we only consider an edge for contraction if, once contracted, it would not create a new edge longer than d_{max}.

This algorithm has one main weakness: it may remove meaningful details if they are smaller than d_{max}. To solve this issue, we use the geometrical interpretation of the quadric error metric: it measures the distance to the lines formed by neighboring edges. Therefore, in order to keep small details, we add a second constraint to mark an edge e as eligible: we ask for its contraction error to be under a given threshold err_{max}.

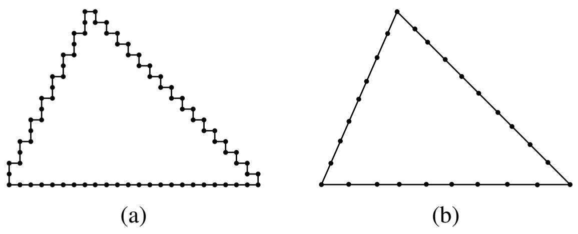

Figure 4: The two substeps of the dense contour extraction phase. (a) The border of the image content is extracted, producing a perfectly accurate shape. (b) This shape is simplified to smooth out staircase artifacts. The density constraint imposes that all edges are smaller than d_{max}.

5 CONTOUR MATCHING

The second step of our algorithm is the matching of vertices between consecutive frames. Consider a frame $0 \leq f < F$, we denote the dense contour extracted from I_f as $C_f = \{v_{f,0}, ..., v_{f,n_f-1}\}$ where each $v_{f,i}$ is a vertex of the dense contour polygon, interpreted as a 2D point. For $0 \leq f < F-1$, the problem of matching C_f with C_{f+1} can be seen as finding for each $v_{f,i}$ a corresponding vertex $v_{f+1,j}$. Note that this matching is asymmetric, however this can be corrected by also matching C_{f+1} with C_f: this will ensure that reading the sequence forward or backward will lead to the same result.

An intuitive way to match $v_{f,i}$ would be to find its nearest neighbor in C_{f+1}. However this approach lacks robustness and leads to unwanted results in many simple cases. Since we are trying to vectorize a coherent object moving across a sequence of images, we can assume that its displacement from one frame to the next one is "small". We approximate this small displacement by a rigid transform on the dense contours. Therefore we can apply a rigid point-set registration technique to find a rigid transform $T : \mathbb{R}^2 \to \mathbb{R}^2$ that best fits C_f onto C_{f+1}. Once we have T, we can match $v_{f,i}$ with C_{f+1} by finding its nearest neighbor in $T^{-1}(C_{f+1})$.

To perform the rigid point-set registration we use the ICP algorithm (Besl and McKay, 1992), and we denote by n_{iter} the number of ICP iterations. This method has the advantage of being fast and simple to implement. In the case where the displacements between consecutive contours cannot be approximated by rigid transforms, we can replace the ICP with more generic point-set registration methods, such as Coherent Point Drift (Myronenko and Song, 2010).

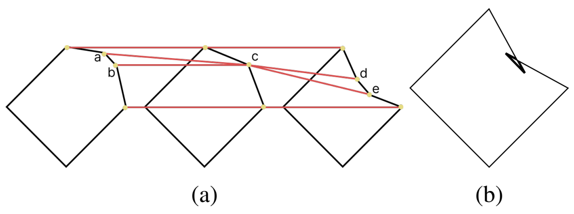

Figure 5: In a situation like the one depicted in (a), the untangling algorithm should favor selecting the animated vertices $a \to c \to d$ and $b \to c \to e$ over $a \to c \to e$ and $b \to c \to d$. Indeed, in the second scenario the animated vertices are crossing each other, resulting in a *twist* artifact as depicted in (b).

6 UNTANGLING

The third step of our algorithm consists in untangling the matches, i.e. extracting an animated cycle from the Tutrace complex we have built so far.

Since the objective of this step is to only change how the data is structured, we wish to minimize its impact on the final geometry, i.e. keep as many animated vertices as possible, well spread over the entire shape. However we cannot simply keep *all* the animated vertices as some of them can "cross" each other, as shown in Figure 5. In this section we present an *ad-hoc* method for extracting animated vertices which ensures that there will be no such artifact in the animated cycle.

6.1 Generating Animated Vertices

One way to build animated vertices from the input data is to compute paths of key vertices connected with temporal edges. Each path should start at the first frame and end at the last frame. The corresponding animated vertices thus have one key vertex per frame.

Generating these animated vertices simply amounts to computing all the paths linking a key vertex at the first frame to a key vertex at the last frame, which can be achieved with a graph traversal algorithm. Note that two animated vertices can potentially share one or more key vertices.

6.2 Circular Ordering and Intervals

Having generated this set of animated vertices, the core problem of *untangling* is to select a subset and structure it in a circular sequence.

For a given frame f let's denote by kc_f the input key cycle at f and $(kv_{f,i})_{0 \leq i < N_f}$ its key vertices indexed in circular order. In addition, for a given animated vertex av, let's denote by $av(f)$ the key vertex lying on av at frame f.

Now imagine we select some animated vertices $(av_j)_{0\leq j<N}$, thus forming an animated cycle ac, which can also be seen as a directed graph with animated vertices as nodes and edges inherited from the circular ordering. At frame f, we want the induced subset of key vertices $(av_j(f))_{0\leq j<N}$ to **respect the circular ordering** of kc_f.

Because of the cyclic nature of the problem, we cannot say that a key vertex is *before* or *after* another one. However we can say that a key vertex is *between* two others if it lies on the path of key edges that connects them. We call *key vertex interval* between two key vertices kv and kv' (denoted $[kv, kv']$) the ordered sequence of key vertices which lie between kv and kv'. Similarly, we call *animated vertex interval* between two animated vertices av and av' (denoted $[av, av']$) the ordered sequence of animated vertices which lie on the path from av to av' in ac. Equipped with these new notions, we can now say that ac respects the circular ordering of kc_f if (and only if) for each animated vertex interval $[av, av']$ the induced key vertex sequence at frame f is a sub-sequence of key vertex interval $[av(f), av'(f)]$.

6.3 Divide-and-Conquer Approach

Let's consider a key vertex interval $[a,b]$ and a key vertex $c \in [a,b]$. We can measure its distance to the interval bounds by taking the maximum between the length of the key edge path $a \to ... \to c$ and the key edge path $c \to ... \to b$. Going further, we can define an interval mid-point as a key vertex minimizing the distance to the bounds. This mid-point definition can be extended to animated vertex intervals by taking an animated vertex that minimizes the maximum distance to the bounds over all frames.

Being able to extract a mid-point from an animated vertex interval allows us to split it into two smaller "balanced" parts, and thus provides a way to construct an animated cycle using a divide-and-conquer approach (see Algorithm 1 for pseudo-code). For the initialization, we select an arbitrary animated vertex av_{ref}, add it to the animated cycle ac, and we exceptionally consider that the interval $[av_{ref}, av_{ref}]$ contains all the generated animated vertices. Then, for each considered interval, we select a mid-point, add it to ac in-between the interval bounds - thus naturally creating the circular order of ac and respecting the circular order of the key cycles - and recursively continue on the two sub-intervals created. The termination condition for the recursion is met when the interval is only constituted of its own bounds.

```
Data: $AV$: set of animated vertices
Result: $ac$: animated cycle
$ac :=$ empty circular list;
$Q :=$ empty FIFO structure;
$av_{ref} :=$ arbitrary element of $AV$;
insert $av_{ref}$ in $ac$;
append $(av_{ref}, av_{ref}, AV)$ to $Q$;
while $Q$ is not empty do
    $av_{start} :=$ animated vertex;
    $av_{end} :=$ animated vertex;
    $I :=$ animated vertex interval;
    pop $1^{st}$ element of $Q$ into
      $(av_{start}, av_{end}, I)$;
    if $I$ contains only $av_{start}$ and $av_{end}$ then
        continue to the next iteration;
    end
    find mid-point $av_{mid} \in I$ that minimizes
      the maximum distance to $av_{start}$ and
      $av_{end}$;
    insert $av_{mid}$ in $ac$ between $av_{start}$ and
      $av_{end}$;
    append $(av_{start}, av_{mid}, [av_{start}, av_{mid}])$ to
      $Q$;
    append $(av_{mid}, av_{end}, [av_{mid}, av_{end}])$ to $Q$;
end
```

Algorithm 1: Pseudo-code for animated cycle extraction from the generated animated vertices during untangling.

7 PRUNING

The fourth step of the algorithm is the simplification of the animated cycle generated during the untangling step. We can perform two kinds of operations to simplify an animated shape: either remove an animated vertex or remove a keyframe (i.e. all the key vertices at a given frame). We divide this step into two distinct pass: a *spatial* pass that removes animated vertices, and a *temporal* pass that removes keyframes.

7.1 Spatial Pruning

In the spatial pruning pass, we interpret the animated cycle as a directed circular graph where the nodes are the animated vertices. We then apply an algorithm similar to what is done in Potrace (Selinger, 2003):

1. we assign to each edge a weight w_{base}
2. for each path $u \to ... \to v$ in the original graph of length at most l_{max} we create a new directed edge $u \to v$ and assign it a weight equal to w_{base} plus the maximum geometric error made by short-cutting the path $u \to ... \to v$ with the path $u \to v$ over all frames

Table 1: Description of evaluation dataset.

Name	Dim	Frames	Source
airplane	1920x1080	50	Synthetic
birdfall	259x327	30	SegTrack V2
blackswan	1920x1080	50	DAVIS 2017
cactus	720x1080	30	Synthetic
car-shadow	1920x1080	40	DAVIS 2017
house	640x480	20	Synthetic
parachute	414x352	51	SegTrack V2
paragliding	1920x1080	70	DAVIS 2017
penguin	384x212	42	SegTrack V2
rallye	1920x1080	50	DAVIS 2017
shark	1080x720	30	Synthetic
sheep	1920x1080	68	DAVIS 2017
statue	640x480	20	Synthetic
worm	480x264	244	SegTrack V2

3. we compute a circuit in this graph that minimizes the sum of weights, which becomes the new animated shape.

The main idea behind this algorithm is that we will shortcut the redundant vertices in areas that remain flat over the entire animation because the error will be low.

7.2 Temporal Pruning

In the temporal pruning pass, we view the animated cycle as a sequence of F key cycles, and we interpret each key cycle as a vector in $\mathbb{R}^{2n}$ (with n the number of animated vertices) by stacking the position of the animated vertices at a given frame. Using this representation we can apply a generalized version for arbitrary dimension of the Ramer-Douglas-Peucker line simplification algorithm introduced in (Douglas and Peucker, 1973). We will denote by θ_{kf} the error threshold parameter in the RDP algorithm. This technique will produce a set of keyframes to keep in our animated shape, and we can then remove the discarded ones.

The intuition here is that we will remove keyframes in frame ranges where they can be well approximated by linear interpolation.

8 EXPERIMENTAL RESULTS

We evaluated our method on a variety of binary image sequences. Our dataset (Vital, 2024) contains videos coming from 3 different sources, as it allows us to cover a wide range of input properties (see Table 1): synthetic sequences made by rendering only the *matte* layer of 3D objects, sequences coming from the SegTrack V2 dataset (Li et al., 2013) and sequences coming from the DAVIS 2017 dataset (Pont-Tuset et al., 2017).

Table 2: Rasterization error comparison. Rasterization errors have been mutliplied by 10^4 for readability.

Name	Potrace	VTracer	Tutrace
airplane	96	4	5
birdfall	37	4	13
blackswan	275	7	11
car-shadow	96	3	13
house	35	16	25
parachute	67	6	10
paragliding	38	0	2
penguin	81	13	22
rallye	35	1	11
shark	239	11	21
sheep	133	2	4
statue	188	9	16

8.1 Comparison with Frame-by-Frame Vectorization

We compare our results to what would be obtained by vectorizing each frame independently. The output of such a process is not an animated vector shape but a sequence of static vector shapes, however we can still compare the *rasterization error*, i.e. the per-pixel difference between the input images and the images obtained by rasterizing the vector shapes.

For the comparison, we use two different vectorization algorithms: Potrace (Selinger, 2003) which has been in use for years in software such as Inkscape, and VTracer (Pun and Tsang, 2020) which is a more recent alternative to Potrace. For Potrace, we set the α_{max} parameter to 0 to generate only polygonal outputs, and we disable the curve optimization. Similarly for VTracer we set the output mode to "polygon". For Tutrace, we use the following parameters: $d_{max} = 20$, $err_{max} = 2$, $n_{iter} = 20$, $l_{max} = 5$, $w_{base} = .5$, and $\theta_{kf} = 3$.

It is important to note that even though these tests provide a good basis for comparison, comparing two different structures has some limitations: for instance, we cannot use the number of keyframes in the animated vector shape as a metric, even though it is an important factor in the final quality.

The evaluation results are displayed in Table 2, which shows that our method performs quite well in terms of rasterization error: the results are not as good as VTracer, but this was expected since frame-by-frame vectorization has no temporal constraint to satisfy, however we still out-perform Potrace on every sequence.

The number of animated vertices generated by

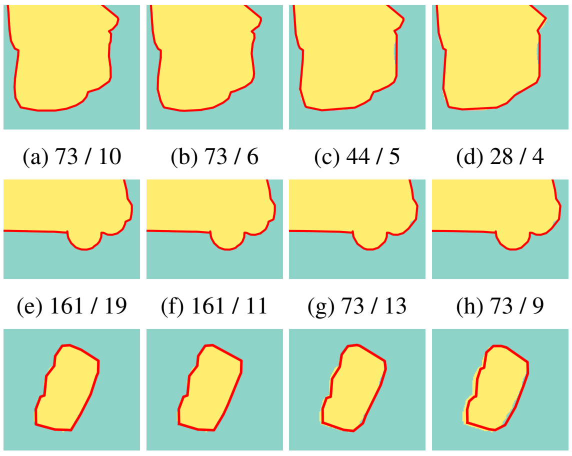

(a) 73 / 10 (b) 73 / 6 (c) 44 / 5 (d) 28 / 4

(e) 161 / 19 (f) 161 / 11 (g) 73 / 13 (h) 73 / 9

(i) 35 / 23 (j) 20 / 12 (k) 20 / 9 (l) 20 / 4

Figure 6: Varying pruning parameters on the “statue”, “car-shadow” and “parachute” sequences to generate simpler outputs. Figures are annotated like so: number of animated vertices / number of keyframes.

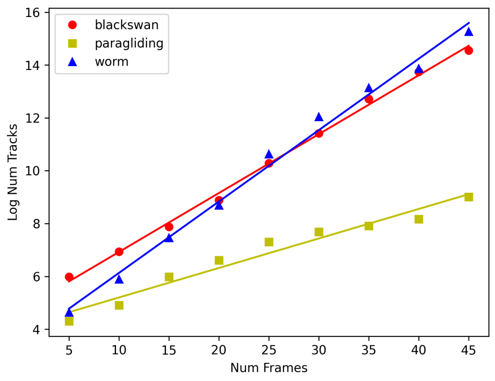

Figure 7: For the “blackswan”, “paragliding” and “worm” sequences, we restricted the sequence to a given number of frames and computed the number of animated vertices to generate during the untangling step. We display the logarithm of that number, along with a linear approximation to highlight its exponential growth.

our method is comparable to the average number of vertices generated by Potrace but generally higher than VTracer. Once again this was expected since our method has to account for changing geometry throughout the animation. However if we consider the output complexity, i.e. the total number of control points used to define the shapes, we remark that Tutrace is more compact than Potrace on all sequences, and more compact than VTracer on all sequences except 3, namely “blackswan”, “paragliding” and “rallye”.

This experimental comparison shows that, in addition to generating a very specific and constraining geometric structure, Tutrace offers a good compromise between output quality and complexity.

8.2 Fidelity vs. Simplicity Trade off

The final *pruning* step of our method offers the possibility to control the complexity of the generated animated shape. The less complex an animated shape is, the larger the rasterization error. However in some applications it can be beneficial to be able to generate coarser shapes, as they are easier to work with. As shown in Figure 6, by manipulating the pruning parameters one can obtain various levels of simplification and thus easily generate a shape with the appropriate complexity.

8.3 Limitations and Failure Cases

As can be seen in Table 2, two sequences from the dataset were not present in the comparison: *cactus* and *worm*. As explained in more details below, these sequences reached the limits of what can currently be achieved with Tutrace.

When working on the *worm* sequence (which is particularly long), we have found that the impact of the number of frames is critical for the performance of the algorithm. Indeed, since the matching step does not always produce 1-1 correspondences between key vertices in adjacent frames, some animated vertices generated at the beginning of the untangling step will “split” at each new frame, leading to a combinatorial explosion. We measured the number of animated vertices generated until a given frame for several sequences in our dataset. The results are shown in Figure 7. As we can see, the growth can be well approximated by an exponential growth, with a coefficient that varies from one sequence to another.

As for the *cactus* sequence, it is part of the synthetic sequences made specifically for these experiments: it consists of a static 3D cactus model around which the camera is turning. As can be seen in Figure 8, the particular shape of the cactus will generate many occlusions, with branches appearing, disappearing and reappearing. Even though the Tutrace algorithm was designed to handle occlusions - such as the nose on the *statue* sequence shown in Figure 1 - this particular case is too complex to untangle for our system: when a side branch merges into the central trunk, the empty region between that branch and the trunk shrinks and disappears quickly, however the particular elongated shape of that region makes it difficult for vertices to get matched properly as they will end up matching against the outer side of the branch instead, thus creating erroneous animated vertices. Note that in practice, rotoscoping artists would not work on the

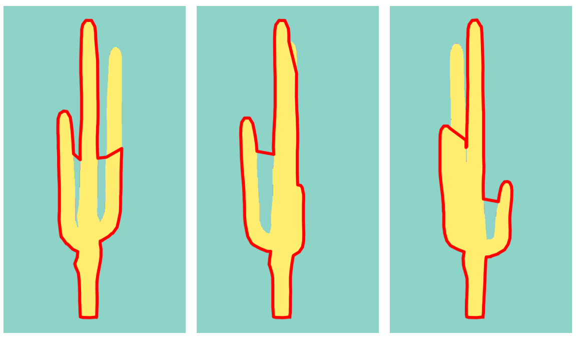
Figure 8: A failure case with the "cactus" sequence.

whole cactus shape at once: they would work on each branch separately to tackle this occlusion problem.

9 FUTURE WORK

As mentioned previously, an important limitation of our method is performance, mostly due to the number of animated vertices that we generate during the untangling step which can increase quickly with the number of frames. We see two main ways to overcome this issue in the future: modify the untangling algorithm to generate only the necessary animated vertices and/or cut down the input video into smaller chunks which will be processed independently and then merged.

We could also try to reinterpret the untangling problem as a multi-graph matching task, where the graphs to match would simply be the key cycles. Indeed, many advancements have been made in recent years on this topic (Yan et al., 2016), which would allow us to solve the untangling step much faster and without requiring an *ad-hoc* method. However such algorithms are designed to extract collections of corresponding nodes in the input graphs, which can be interpreted in our setting as animated vertices, but not the *structure* relating these collections to each other, i.e. the circular structure of an animated cycle in our case. Further work would therefore be required to see if we could extend a multi-graph matching method to fit our purposes.

Another important topic to investigate is *smoothing*. Indeed, the shape we currently generate only contains straight line segments, whereas most image vectorization methods produce smooth shapes, using for instance Bézier segments. Smoothing an animated vector shape is not a trivial problem, however it would also have another positive side effect: fewer vertices would be required to accurately vectorize curved areas in the input images. (Shao and Zhou, 1996) proposes a curve fitting algorithm that could potentially fit our purposes, if we could properly adapt the identification of critical points to animated vertices.

It can also be noted that in our pipeline the images are only fed into the first step, and never used again. Re-using the input images later in the process could allow us to improve the quality of the animated shape by fitting its geometry to the input data. Some methods for optimizing the rasterization error of a vector shape have been proposed, such as (Li et al., 2020), which could be extended to include the temporal dimension of video vectorization.

Handling multiple objects and occlusions could also have a major impact, as these types of situations arise frequently in rotoscopy, for instance when several characters interact in the scene. Building on the work of (Zhang et al., 2023) could be an interesting starting point as they provide a framework for solving both object tracking and layer decomposition.

10 CONCLUSION

We have presented a video vectorization algorithm that works on a binarized input and generates an animated vector shape. The core of our method lies in the *untangling* step, which extracts animated vertices from static shapes and correspondences between their vertices. We showed that the output quality is comparable to frame-by-frame vectorization, with the advantage of being directly ready to import and edit in a DCC. Additionally, the user can control the complexity of the animated shape, thus allowing to create simpler shapes. We hope that this method, with the flexible multi-step approach it uses, will serve as a basis for further development in this area, mostly targeting use cases in rotoscopy for VFX.

ACKNOWLEDGEMENTS

Many thanks to Vincent Demoulin for his useful comments and feedback on both Tutrace and this article. We also thank the anonymous reviewers for helping us improve this paper. This work was partially supported by Technicolor Group.

REFERENCES

Besl, P. J. and McKay, N. D. (1992). Method for registration of 3-d shapes. In *Sensor fusion IV: control paradigms and data structures*, volume 1611, pages 586–606. Spie.

Dalstein, B., Ronfard, R., and Van De Panne, M. (2015). Vector graphics animation with time-varying topology. *ACM Transactions on Graphics (TOG)*, 34(4):1–12.

Douglas, D. H. and Peucker, T. K. (1973). Algorithms for the reduction of the number of points required to represent a digitized line or its caricature. *Cartographica: the international journal for geographic information and geovisualization*, 10(2):112–122.

Favreau, J.-D., Lafarge, F., and Bousseau, A. (2016). Fidelity vs. simplicity: a global approach to line drawing vectorization. *ACM Transactions on Graphics (TOG)*, 35(4):1–10.

Garland, M. and Heckbert, P. S. (1997). Surface simplification using quadric error metrics. In *Proceedings of the 24th annual conference on Computer graphics and interactive techniques*, pages 209–216.

Kopf, J. and Lischinski, D. (2011). Depixelizing pixel art. In *ACM SIGGRAPH 2011 papers*, pages 1–8.

Li, F., Kim, T., Humayun, A., Tsai, D., and Rehg, J. M. (2013). Video segmentation by tracking many figure-ground segments. In *Proceedings of the IEEE International Conference on Computer Vision*, pages 2192–2199.

Li, T.-M., Lukáč, M., Gharbi, M., and Ragan-Kelley, J. (2020). Differentiable vector graphics rasterization for editing and learning. *ACM Transactions on Graphics (TOG)*, 39(6):1–15.

Li, Y., Wang, C., Hong, J., Zhu, J., Guo, J., Wang, J., Guo, Y., and Wang, W. (2021). Video vectorization via bipartite diffusion curves propagation and optimization. *IEEE Transactions on Visualization and Computer Graphics*, 28(9):3265–3276.

Myronenko, A. and Song, X. (2010). Point set registration: Coherent point drift. *IEEE Transactions on Pattern Analysis and Machine Intelligence*, 32(12):2262–2275.

Orzan, A., Bousseau, A., Winnemöller, H., Barla, P., Thollot, J., and Salesin, D. (2008). Diffusion curves: a vector representation for smooth-shaded images. *ACM Transactions on Graphics (TOG)*, 27(3):1–8.

Pont-Tuset, J., Perazzi, F., Caelles, S., Arbeláez, P., Sorkine-Hornung, A., and Van Gool, L. (2017). The 2017 davis challenge on video object segmentation. *arXiv preprint arXiv:1704.00675*.

Pun, S. and Tsang, C. (2020). Vtracer. https://www.visioncortex.org/vtracer-docs.

Selinger, P. (2003). Potrace: a polygon-based tracing algorithm.

Shao, L. and Zhou, H. (1996). Curve fitting with bezier cubics. *Graphical models and image processing*, 58(3):223–232.

Sun, J., Liang, L., Wen, F., and Shum, H.-Y. (2007). Image vectorization using optimized gradient meshes. *ACM Transactions on Graphics (TOG)*, 26(3):11–es.

Vital, L. (2024). Tutrace evaluation videos. {https://doi.org/10.5281/zenodo.14510189}.

Wang, C., Zhu, J., Guo, Y., and Wang, W. (2017). Video vectorization via tetrahedral remeshing. *IEEE Transactions on Image Processing*, 26(4):1833–1844.

Xia, T., Liao, B., and Yu, Y. (2009). Patch-based image vectorization with automatic curvilinear feature alignment. *ACM Transactions on Graphics (TOG)*, 28(5):1–10.

Yan, J., Yin, X.-C., Lin, W., Deng, C., Zha, H., and Yang, X. (2016). A short survey of recent advances in graph matching. In *Proceedings of the 2016 ACM on International Conference on Multimedia Retrieval*, pages 167–174.

Yao, R., Lin, G., Xia, S., Zhao, J., and Zhou, Y. (2020). Video object segmentation and tracking: A survey. *ACM Transactions on Intelligent Systems and Technology (TIST)*, 11(4):1–47.

Yu, Y., Wang, C., Fu, Q., Kou, R., Huang, F., Yang, B., Yang, T., and Gao, M. (2023). Techniques and challenges of image segmentation: A review. *Electronics*, 12(5):1199.

Zhang, S., Ma, J., Wu, J., Ritchie, D., and Agrawala, M. (2023). Editing motion graphics video via motion vectorization and transformation. *ACM Transactions on Graphics (TOG)*, 42(6):1–13.

Zhang, S.-H., Chen, T., Zhang, Y.-F., Hu, S.-M., and Martin, R. R. (2009). Vectorizing cartoon animations. *IEEE Transactions on Visualization and Computer Graphics*, 15(4):618–629.